Electronic Band Structure and Fermi Surface of CaB_6 Studied by Angle-Resolved Photoemission Spectroscopy

S. Souma,[1] H. Komatsu,[1] T. Takahashi,[1] R. Kaji,[2] T. Sasaki,[2] Y. Yokoo,[2] and J. Akimitsu[2]

[1]*Department of Physics, Tohoku University, Sendai 980-8578, Japan*

[2]*Department of Physics, Aoyama-Gakuin University, Chitosedai, Setagaya-ku, Tokyo 157-8572, Japan*

(Received 3 September 2002; published 15 January 2003)

We report high-resolution angle-resolved photoemission spectroscopy (ARPES) on CaB_6. The band structure determined by ARPES shows a 1 eV energy gap at the X point between the valence and the conduction bands. We found a small electron pocket at the X point, whose carrier number is estimated to be (4–5) $\times 10^{19}$ cm^{-3}, in good agreement with the Hall resistivity measurement with the same crystal. The experimental results are discussed in comparison with band structure calculations and theoretical models for the high-temperature ferromagnetism.

DOI: 10.1103/PhysRevLett.90.027202 PACS numbers: 75.50.Cc, 71.18.+y, 71.20.–b, 79.60.Bm

$Ca_{1-x}La_xB_6$ has attracted much attention because of the anomalous ferromagnetism: (1) it contains no "magnetic" ions, (2) the Curie temperature (600 K) is remarkably high, but (3) the magnetic moment is extremely small ($0.07\mu_B$/La atom), and (4) the appearance of the ferromagnetism is restricted to a very narrow doping region [1,2]. Two different theoretical approaches to understand the high-temperature ferromagnetism have been proposed, the excitonic-insulator model [3–6] and the low-density electron-gas model [7,8]. The former is based on the electron-hole excitation (excitons) near the Fermi level (E_F) in a small region of the Brillouin zone, which requires an intrinsic semimetallic nature of the parent compound (CaB_6). The overlap of an electron and a hole pocket at E_F is essential for the formation of excitons in the model. The LDA (local-density-approximation) band calculation has predicted the semimetallic nature of CaB_6 with a small overlap of an electron and a hole band at X point in the Brillouin zone [9–11], in support of the excitonic-insulator model. In contrast, the LDA + GW band calculation has reported that a relatively large energy gap opens at X point in CaB_6 when the self-energy correction is appropriately included in the calculation, proposing that CaB_6 is intrinsically semiconductive [12].

On the experimental side, there is also considerable confusion regarding the metallic/nonmetallic nature of CaB_6. The semimetallic nature is supported by the metallic resistivity [13,14], the de Haas–van Alphen signal [13,15], and the plasma edge in the optical spectrum [16–18]. On the other hand, NMR [19], angle-resolved photoemission spectroscopy (ARPES) [20], and the thermopower experiment [21] suggest that CaB_6 is a wide-gap semiconductor. In order to resolve the confusion in the theory and experiment and to reveal the mechanism of the high-temperature ferromagnetism in doped CaB_6, it is necessary to experimentally establish the electronic structure near E_F.

In this Letter, we report results of high-resolution ARPES on CaB_6. We have experimentally determined the valence-band structure of CaB_6 and compare the results with the two different band structure calculations, LDA [10] and LDA + GW calculations [12]. By using ultrahigh resolutions in the energy and momentum, we have succeeded in directly observing a small electronlike spheroidal Fermi surface at X point in the Brillouin zone. We found that the volume of the Fermi surface, namely, the carrier number, shows an excellent quantitative agreement with Hall resistivity measurement with the same crystal. We compare the ARPES results with two different theoretical models, the excitonic-insulator model [3–6] and the low-density electron-gas model [7,8], and discuss the possible mechanism of the anomalous high-temperature ferromagnetism in doped CaB_6.

CaB_6 single crystals were grown by the floating zone method. As shown in Fig. 1, the grown crystal shows a weak but distinct ferromagnetic behavior at room temperature as well as the metallic nature in the electrical resistivity down to low temperature. We also performed Hall resistivity measurements to compare with the

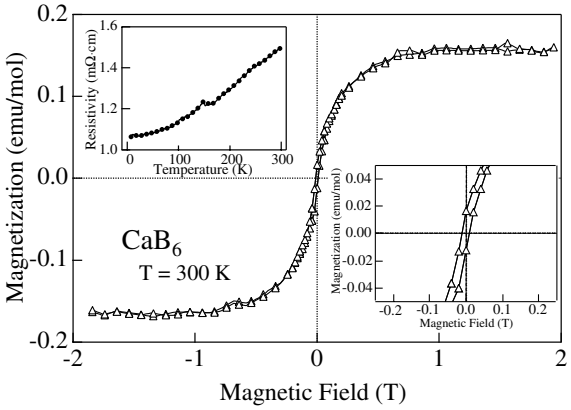

FIG. 1. Magnetization curve of CaB_6 single crystal used in the present study. Insets show the expansion of magnetization curve near zero field (lower right) and the electrical resistivity as a function of temperature (upper left).

ARPES result. ARPES measurements were performed using a GAMMADATA-SCIENTA SES-200 spectrometer with a high-flux discharge lamp and a toroidal grating monochromator. The energy and momentum resolutions were set at 20 meV and 0.01 $Å^{-1}$, respectively. The crystal orientation was determined by Laue x-ray diffraction prior to the ARPES measurements. The crystal was cleaved *in situ* along the (001) plane at 30 K in a vacuum of 3×10^{-11} Torr. The Fermi level of the sample was referred to a gold film evaporated on the sample substrate. We have performed ARPES measurements with six different cleaves/crystals and confirmed the reproducibility of the data.

Figure 2(a) shows valence-band ARPES spectra of CaB_6 measured along the [100] (ΓX) direction with the He Iα resonance line (21.218 eV) at 30 K. Figure 2(b) shows the expansion of the same spectra near E_F. Prominent structures in the valence-band ARPES spectra, which show a systematic dispersion in the binding energy of 1–4 eV, are ascribed to the B $2p$-$2s$ hybridized states of B_6 octahedron in the crystal. We also find additional small structures in the higher binding-energy region, also ascribable to the B $2p$-$2s$ states with a relatively higher B $2s$ weight. In contrast, no or negligible features are seen in the vicinity of E_F in the intensity scale of Fig. 2(a), although the expansion of spectra near E_F suggests a small structure around the X point. We discuss this small structure in detail later.

Figure 3 shows the ARPES-derived "band structure" of CaB_6, which is obtained by taking the second derivative of ARPES spectra in Fig. 2(a) after moderate smoothing and plotting the intensity as a function of the wave vector and the binding energy. The bright areas correspond to the experimental bands. The dispersion of experimental bands matches quite well with the periodicity of the bulk Brillouin zone, suggesting that the peaks/structures in the ARPES spectra originate in the bulk electronic structure, in particular, from the high-symmetry lines in the bulk Brillouin zone, ΓX and XM [22]. The experimental result in Fig. 3 is consistent with the previous ARPES study [20]. Figure 3 also shows comparison of the ARPES-derived band structure with two different band calculations, LDA [10] and LDA + GW [12].

It is obvious that the LDA band calculation is shifted as a whole toward E_F with respect to the experiment, although the gross feature in the band dispersions looks similar. The fatal disagreement lies in the region near E_F at the X point, where the LDA calculation predicts a dispersive band which forms a hole pocket at the X point while the corresponding experimental band is situated far away (about 1 eV) from E_F at the X point. In contrast, the LDA + GW calculation is found to be in good agreement with the ARPES result; a highly dispersive band from $\Gamma(X)$ to $X(M)$ shows an almost perfect agreement, and a relatively flat band near E_F around the X point is qualitatively well reproduced in the calculation. The present study unambiguously shows that the band structure obtained by ARPES reflects the bulk property because (1) the measured band dispersion periodicity matches well with that of the bulk Brillouin zone, and (2) the

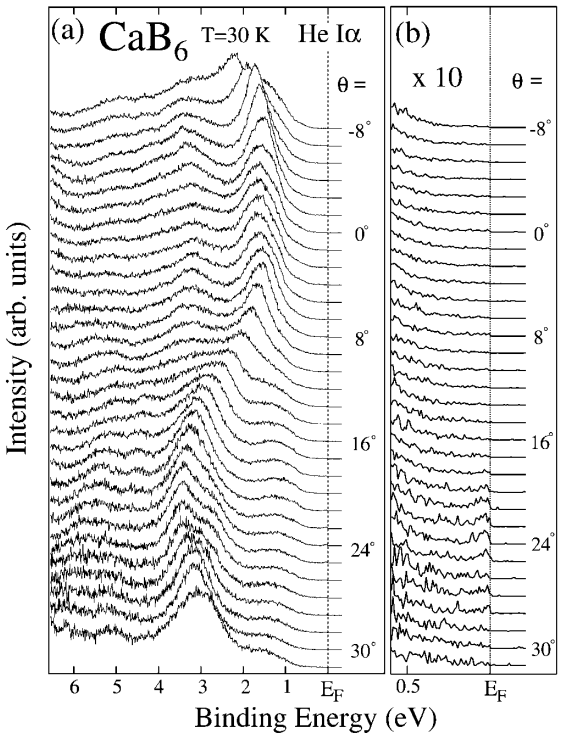

FIG. 2. (a) Valence-band ARPES spectra of CaB_6 along the ΓX direction in the Brillouin zone measured with He Iα photons (21.218 eV) at 30 K. Polar angle (θ) referred to the surface normal is indicated. (b) Expansion of the spectra near E_F.

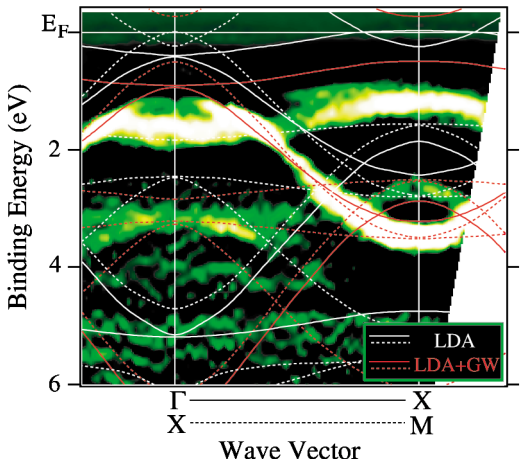

FIG. 3 (color). Experimental band structure of CaB_6 along the ΓX direction determined by ARPES. Bright areas correspond to bands. LDA [10] and LDA + GW [12] band calculations are also shown by white and red lines, respectively, for comparison.

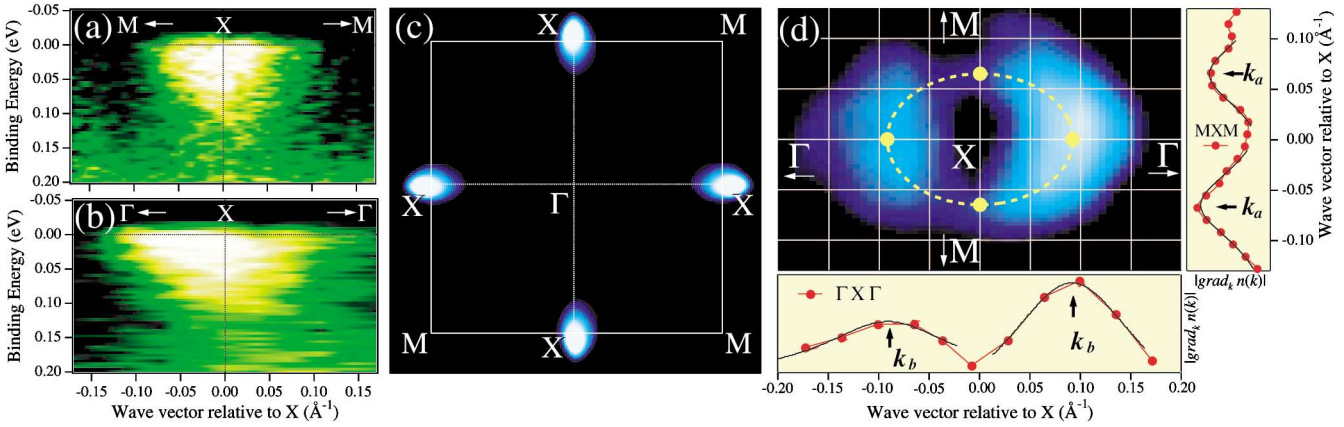

FIG. 4 (color). (a),(b) Plots of ARPES intensity near E_F around the X point in two directions, MXM and $\Gamma X\Gamma$. (c) Location and shape of Fermi surface of CaB_6 determined by plotting the ARPES intensity integrated from -20 meV to $+20$ meV with respect to E_F. (d) Intensity map of $|\mathrm{grad}_{\mathbf{k}}\, n(\mathbf{k})|$ together with $|\mathrm{grad}_{\mathbf{k}}\, n(\mathbf{k})|$ cut along $\Gamma X\Gamma$ (bottom panel) and MXM (right panel). Broken yellow lines trace k_F positions determined from the local maximum of $|\mathrm{grad}_{\mathbf{k}}\, n(\mathbf{k})|$.

carrier number estimated from ARPES shows a quantitatively good agreement with the Hall resistivity measurement. The latter will be discussed in detail later. Thus, the present ARPES result shows that a large (1 eV) gap opens between the conduction and the valence bands at the X point in CaB_6.

The next question is whether this energy gap is an intrinsic semiconducting gap as predicted from the LDA + GW calculation [12] or an energy gap created by the formation of excitons (excitonic-insulator gap) as proposed by the excitonic-insulator model [3–6]. According to the theory [3–6], the energy of the excitonic-insulator gap is comparable to the transition temperature of ferromagnetism, 600 K (= 50 meV) [1,2]. In contrast, as shown in Fig. 3, the observed gap has an energy of 1 eV, which corresponds to 12 000 K. This large difference in the energy scale indicates that the 1 eV energy gap at the X point is an intrinsic semiconducting energy gap, not due to the formation of excitons. A large energy gap between the conduction and the valence bands has also been suggested by the previous ARPES and x-ray spectroscopy [20].

The observed large semiconducting gap seems to apparently contradict the metallic nature of the sample shown in Fig. 1. However, this discrepancy may be resolved by the small structure near E_F around the X point as shown in Fig. 2(b). In order to study the detailed electronic structure near E_F, we have measured ARPES spectra along many cuts in the Brillouin zone and found that this small structure is localized around the X point. Figures 4(a) and 4(b) plot the ARPES intensity near E_F around the X point in the two directions, XM and $X\Gamma$, respectively, where we clearly find a small dispersive feature indicating a small electronlike Fermi surface centered at the X point. The ARPES intensity distributes more widely in the $X\Gamma$ direction than in the XM direction, indicative of a spheroidal shape of the Fermi surface. This is more clearly seen in Fig. 4(c) where the ARPES intensity near E_F ($\pm$ 20 meV with respect to E_F) is plotted in the two dimensional Brillouin zone. Figure 4(c) clearly shows that the CaB_6 single crystal used in the present ARPES measurement has a small electronlike spheroidal Fermi surface elongated along the $X\Gamma$ direction centered at the X point. This means that the CaB_6 crystal is already doped, probably due to defects or deficiencies in the crystal. In return, this small Fermi surface gives the metallic nature to the sample, consistent with the electrical resistivity shown in Fig. 1.

Next we estimate the volume of the Fermi surface, namely, the carrier number, from the ARPES experiment. Figure 4(d) shows the intensity of $|\mathrm{grad}_{\mathbf{k}}\, n(\mathbf{k})|$, where $n(\mathbf{k})$ is the momentum distribution function defined with the ARPES spectral intensity near E_F integrated from 50 meV above E_F to 150 meV below E_F. We have estimated the Fermi vectors measured from the X point in the XM and $X\Gamma$ directions (k_a and k_b) by taking the maximum point of $|\mathrm{grad}_{\mathbf{k}}\, n(\mathbf{k})|$ [23] as shown in Fig. 4(d). They are 6.5×10^{-2} Å^{-1} and 9.2×10^{-2} Å^{-1} for the shorter (k_a) and longer (k_b) axes, respectively. By assuming a perfect spheroidal shape, we have estimated the volume of the Fermi surface to be 2.8×10^{-3} of the whole Brillouin-zone volume, which corresponds to the carrier number of 3.9×10^{19} cm^{-3}. In order to independently estimate the character and the number of carriers, we also performed Hall resistivity measurements with the same crystal as used in the ARPES measurement. It is important to compare the ARPES result with the bulk transport property. The Hall resistivity measurement shows that the sign of the carrier is negative and the number of the carrier at 30 K is 5.2×10^{19} cm^{-3}, which shows an excellent agreement with the ARPES result. All these indicate that the CaB_6 single crystal used in the

present study has a small electronlike spheroidal Fermi surface centered at the X point in the Brillouin zone and the volume (carrier number) is $(4–5) \times 10^{19}$ cm^{-3}.

Finally, we discuss possible mechanisms for the novel ferromagnetism in doped CaB_6 based on the present ARPES results. The band structure determined by ARPES (Fig. 3) clearly shows that a large (1 eV) intrinsic gap opens between the conduction and the valence bands at the X point in the Brillouin zone. This is in sharp contrast to the essential starting point of the excitonic-insulator model [3–6], which assumes overlap of an electron and a hole pocket at E_F. The 1 eV energy gap is hardly accounted for in terms of the formation of excitons. In contrast, the present ARPES results seem to favor the low-density electron-gas model [7,8]. In fact, the obtained carrier density [$(4–5) \times 10^{19}$ cm^{-3}] lies in the predicted polarized-fluid region (10^{18}–10^{20} cm^{-3}) between the Fermi-liquid and the Wigner-crystal regions [7,8]. A remaining problem is how the electrons in the small Fermi surface with a strongly anisotropic t_{2u} molecular-orbital nature give rise to the high-temperature ferromagnetism as almost free electrons in the low-density electron-gas model [7,8].

In conclusion, the present ARPES study on CaB_6 has revealed a large (1 eV) intrinsic energy gap at the X point between the conduction and the valence bands as well as a small electronlike spheroidal Fermi surface at the X point. The experimentally determined band structure as well as the 1 eV energy gap are in good agreement with the LDA + GW band calculation [12], but not with the LDA calculation [10]. The absence of overlap of an electron and a hole Fermi surface in CaB_6 strongly suggests that the ferromagnetism in doped CaB_6 is not accounted for by the formation of excitons [3–6]. The estimated carrier number in the small Fermi surface at the X point lies in the region where the spin polarization of electrons is predicted in the low-density electron-gas model [7,8].

The authors thank Professor Y. Kuramoto for his useful discussion. We also thank H. Kumigashira, T. Ito, T. Sato, and T. Matsumura for their collaboration in measurements. S. S. thanks JSPS for financial support. This work is supported by a grant from the MEXT of Japan.

[1] D. P. Young *et al.*, Nature (London) **397**, 412 (1999).
[2] H. R. Ott *et al.*, Physica (Amsterdam) **281-282B**, 423 (2000).
[3] M. E. Zhitomirsky *et al.*, Nature (London) **402**, 251 (1999).
[4] L. Balents and C. M. Varma, Phys. Rev. Lett. **84**, 1264 (2000).
[5] V. Barzykin and L. P. Gor'kov, Phys. Rev. Lett. **84**, 2207 (2000).
[6] S. Murakami *et al.*, Phys. Rev. Lett. **88**, 126404 (2002).
[7] D. Ceperley, Nature (London) **397**, 386 (1999).
[8] G. Ortiz *et al.*, Phys. Rev. Lett. **82**, 5317 (1999).
[9] A. Hasegawa and A. Yanase, J. Phys. C **12**, 5431 (1979).
[10] S. Massidda *et al.*, Z. Phys. B **102**, 83 (1997).
[11] C. O. Rodriguez *et al.*, Phys. Rev. Lett. **84**, 3903 (2000).
[12] H. J. Tromp *et al.*, Phys. Rev. Lett. **87**, 016401 (2001).
[13] T. Terashima *et al.*, J. Phys. Soc. Jpn. **69**, 2423 (2000).
[14] T. Morikawa *et al.*, J. Phys. Soc. Jpn. **70**, 341 (2001).
[15] D. Hall *et al.*, Phys. Rev. B **64**, 233105 (2001).
[16] H. R. Ott *et al.*, Z. Phys. B **102**, 337 (1997).
[17] P. Vonlanthen *et al.*, Phys. Rev. B **62**, 10 076 (2000).
[18] K. Taniguchi *et al.*, Phys. Rev. B **66**, 064407 (2002).
[19] J. L. Gavilano *et al.*, Phys. Rev. B **63**, 140410(R) (2001).
[20] J. D. Denlinger *et al.*, Phys. Rev. Lett. **89**, 157601 (2002).
[21] K. Gianno *et al.*, J. Phys. Condens. Matter **14**, 1035 (2002).
[22] We have also performed similar ARPES measurements with a different photon energy (He IIα, 40.814 eV) and obtained almost the same experimental band dispersion as that with He Iα in Fig. 3. This means that the momentum broadening perpendicular to the surface is substantially large and as a result the ARPES measurement with He Iα (and He IIα) picks up the relatively large density of state on the high-symmetry lines.
[23] Th. Straub *et al.*, Phys. Rev. B **55**, 13 473 (1997).